Physical Sciences

Review article

Structural analysis of the $RE_3Ba_5Cu_8O_{18}$ (RE = Dy, Gd, Ho, Sm, Y, Yb) superconductor system

Análisis estructural del sistema superconductor $RE_3Ba_5Cu_8O_{18}$ (RE = Dy, Gd, Ho, Sm, Y, Yb)

Carlos A. Parra-Vargas[1],*, **Cesar Camilo Canaría-Camargo[1],** **Jairo Roa-Rojas[2],**
José Albino-Aguiar[3]

[1] Grupo de Física de Materiales (GFM), Universidad Pedagógica y Tecnológica de Colombia, Tunja, Colombia
[2] Departamento de Física, Universidad Nacional de Colombia, Bogotá, D.C., Colombia
[3] Centro de Ciências Exatas e da Natureza, Universidade Federal de Pernambuco, Recife, Brazil

Carlos A. Parra-Vargas, Inaugural article for admission as a Corresponding Member to the Academia Colombiana de Ciencias Exactas, Físicas y Naturales

Abstract

In this paper, we report the synthesis and structural characterization of the $RE_3Ba_5Cu_8O_{18}$ (RE = Dy, Gd, Ho, Sm, Y, Yb) system, which adds to the findings reported by **Aliabadi, *et al.,*** who determined a critical temperature (T_C) of ~ 100 K for the superconducting $Y_3Ba_5Cu_8O_{18}$ system and evaluated its structural response in a sample. The new $RE_3Ba_5Cu_8O_{18}$ system was produced using the solid-state reaction method and a similar thermal process as the one used for the superconductor RE: 123. The experimental results obtained with X-ray diffraction and the Rietveld analysis showed that these samples had the expected crystal structure. However, it was obvious that the presence of non-superconducting phases did not affect the superconducting transition temperature. Moreover, magnetic studies revealed that $RE_3Ba_5Cu_8O_{18}$ samples showed a superconductivity transition within a temperature range of 80 - 93 K depending on the rare earth.

Keywords: New superconducting materials; $RE_3Ba_5Cu_8O_{18}$ superconductor; Solid-state reaction.

Resumen

En este artículo reportamos la síntesis y caracterización estructural del sistema $RE_3Ba_5Cu_8O_{18}$ (RE = Dy, Gd, Ho, Sm, Y, Yb), lo que viene a complementar lo ya reportado por **Aliabadi, *et al.,*** quienes lograron una temperatura crítica (T_C) de ~ 100 K para el sistema superconductor $Y_3Ba_5Cu_8O_{18}$, y evaluó la respuesta estructural en una muestra. Asimismo, los resultados experimentales obtenidos mediante la técnica de difracción de rayos X y el análisis de Rietveld evidenciaron que estas muestras tenían la estructura cristalina esperada; sin embargo, fue obvio que la presencia de fases no superconductoras no afectó la temperatura de transición superconductora. Además, los estudios magnéticos revelaron que las muestras de $RE_3Ba_5Cu_8O_{18}$ registraban una transición superconductora en el rango de 80 a 93 K dependiendo de la tierra rara.

Palabras clave: Nuevos materiales superconductores; Superconductor $RE_3Ba_5Cu_8O_{18}$; Reacción de estado sólido.

Introduction

Since high-critical temperature superconductors (HTSCs) were discovered, there have been many attempts to raise the temperature of transition between the normal and the superconducting state. These HTSCs have a simple or a complex perovskite structure *ABO*x depending on the number of rare earths atoms that are arranged in the stoichiometry (**Sandoval-Gutiérrez, *et al.,*** 2015).

Aliabadi, *et al.* (2009) reported the new high-temperature superconductor (HTSC) $Y_3Ba_5Cu_8O_{18}$ (Y358), which reached a temperature above 100 K. Y358 has a crystalline structure similar to that of Y123, with five CuO_2 planes and three CuO chains; this increased number of CuO_2 planes and CuO chains has an important effect on the Tc of Y358 (**Udomsamuthirun, *et al.*,** 2010). Y358 exhibits three Y atoms and five Ba atoms and, hence, eight Cu atoms are obtained (**Landínez-Téllez, *et al.*,** 2015). The ceramic superconductor Y358 has a transition temperature of 101 K, i.e., 10 K above that of any of the YBCO compounds family (**Gholipour, *et al.*,** 2012).

The discovery of the new Y358 superconducting system has allowed for new and important results regarding the phenomenology of the superconducting cuprates. It has been prepared under different growth techniques, such as conventional sintering, sol-gel, and biopolymer-mediated and melt-texturing methods, resulting in different specimens, from polycrystalline samples to super-conducting nanowires. Different compounds have been derived, such as $Yb_{1.8}Sm_{1.2}Ba_5Cu_8O_{18}$, $RE_3Ba_5Cu_8O_{18}$ (RE = Sm and Nd), $Y_3Ba_5Ca_2Cu_8O_{18}$, $Y_3Ba_5Cu_8O_{y-x}F_x$, and $Y_3Ba_5Cu_{8-x}Zn_xO_{18}$ and several studies have compared the YBaCuO family members structural, magnetic, and electric properties (**Dias, *et al.*,** 2014).

Recently, **Aliabadi, *et al.*** (2009), **Tavana, *et al.*** (2010), and **Udomsamuthirun, *et al.*** (2010) demonstrated the new Y-based high-temperature superconductor in Y3Ba5Cu8O18 (Y358) that acquired superconductivity above the 100 K of temperature. They also proposed that to obtain a stronger superconductor with a higher Tc in the YBaCuO family, more holes from the chains to the oxygen sites of the planes tending to diagonal-charge order should be pumped. The Y123 has two CuO2 planes and one CuO chain while Y124 has one CuO double chain, Y247 has one CuO2 plane, one CuO chain, and one double chain. Y358 has a crystalline structure like that of Y123 with five CuO2 planes and three CuO chains. The increase in the number of CuO2 planes and CuO chains has an important effect on the Tc of Y358. The number of CuO2 planes and CuO chains or double chains believed to be the carrier reservoirs differs among YBaCuO family compounds. **Aliabadi, *et al.*** (2009) proposed that the Y123 lattice parameters a and b are very close to those of Y358, but the lattice parameter c of Y358 is almost three times that of Y123. **Udomsamuthirun, *et al.*** (2010) have postulated the following compositional relations for the unit cell: The number of CuO2 planes equals the number of Ba-atoms; the number of CuO chains equals the number of Y-atoms, and 3) the number of Ba-atoms plus Y-atoms equals the number of Cu-atoms.

However, experimentally it can be proved that the number of Ba-atoms plus Y-atoms equals the number of Cu-atoms. In Y123, there is one Y-atom and two Ba-atoms, so we get three Cu-atoms. In Y358, there are three Y-atoms and five Ba-atoms, so we get eight Cu-atoms. According to this approach, to reach the highest Tc, more holes in the CuO2 planes must be pumped. We assume that the number of Y atoms should be missing to create more holes and thus increase the critical temperature. At this point, we can make the following assumptions to synthesize a new superconductor in the YBaCuO family: 1) The number of Ba-atoms plus Y-atoms is equal to the number of Cu-atoms, and 2) the number of Y-atoms can be missing to reach the higher Tc, but then the first assumption should be obeyed.

The Y123 and Y358 can be explained by the assumption that in Y123 there are no Y-atoms missing and in Y358 there is one Y-atom missing for every five Ba-atoms. Based on our assumptions, there should be many new superconductors to be found. For example, in the case of one Y-atom missing, the general formula should be $Y_{x-2}Ba_xCu_{2x-2}O_\delta$. Y358 in this group has the percentage of Y-atoms missing in relation to the number of Ba-atoms, which is expressed as $1/5 \times 100 = 20\%$. For the two Y-atoms missing, the general formula should be $Y_{x-3}Ba_xCu2_{x-3}O_\delta$. We can get Y5813 with the percentage of Y-atoms missing in relation to the number of Ba atoms expressed as $2/8 \times 100 = 25\%$. Additionally, to this analysis, based on the structure reported by **Gholipour, *et al.*** (2012), we report the synthesis and structural analysis of the new $RE_3Ba_5Cu_8O_{18}$ (RE = Dy, Gd, Ho, Sm, Y, Yb) superconductor system.

Materials and methods

The superconductor samples of $RE_3Ba_5Cu_8O_{18}$ doped with RE = (Dy, Gd, Ho, Sm, Y, Yb) were produced using the solid-state reaction method (RSS) with Sigma-Aldrich raw materials of high-purity: $BaCO_3$ (99.999%), CuO (99.999%), Y_2O_3 (99.9%), Dy_2O_3 (99.9%), Sm_2O_3 (99.99%), Gd_2O_3 (99.9%), Ho_2O_3 (99.99%), and Yb_2O_3 (99.99%). The powders were dried at 200 °C for 15 hours, weighed in stoichiometric amounts, then these were macerated for 4 hours in an agate mortar, and the powder obtained was decarbonated at 750 °C for a period of 12 hours in a muffle furnace (**Figure 1**). The powders were macerated and pressed into a double effect cylindrical matrix at 2.5 MPa in a hydraulic press. The mixed materials were then calcined and sintered for 12 hours and 48 hours, respectively, at several temperatures. The samples obtained were pressed into pellets and sintered for 24 hours in an oxygen atmosphere and then cooled to room temperature at a rate of 5 °C/min. The heat treatment processes of the samples were performed in an alumina crucible. Calcined and sintered temperatures were different for the five samples. The various authors expected differences in synthesis temperatures in their studies, but they have shown that crystallization temperatures of the RE-358 compounds vary depending on the ionic radius of the RE^{3+} ion (**Table 1**) (**Topal & Akdogan,** 2012; **Slimani,** *et al.,* 2018).

X-ray diffraction (XRD) patterns taken at room temperature were used to identify the crystalline structure of the five samples. The XRD pattern was obtained with a Panalytical X´pert PRO-MPD equipment with an ultrafast X'Celerator detector in Bragg-Brentano
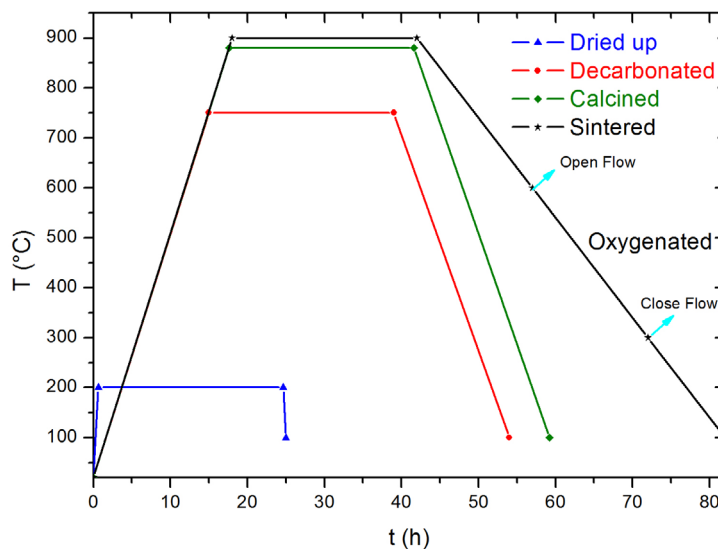
Figure 1. Temperature ramps

Table 1. Calcined and sintered temperatures for the RE-358 system

Sample	Calcination temperature (°C)	Sintering temperature (°C)
Sm-358	800	850
Gd-358	830	880
Dy-358	830	880
Ho-358	800	850
Y-358	830	880
Yb-358	830	870

configuration using CuKα radiation (λ = 1.5418 Å). The patterns were scanned for a 2θ scattering angle between 15° and 90°, a step value of 0.0263°, and a counting time of 100 s. The XRD patterns were analyzed with the General Structure Analysis System (GSAS©) software. The magnetic-property samples were examined using the Quantum Design VSM system with the routine ZFC - ZFC (Zero Field Cooled - Field Cooled) between 50 K and 300 K and magnetic fields from 100 Oe to 8000 Oe.

Results and discussion

The $RE_3Ba_5Cu_8O_{18}$ systems were analyzed from crystallographic databases. The theoretical model used to compare the superconducting samples (**Table 2**) has been tested on similar systems (**Pimentel, *et al.***, 2015; **Topal, *et al.***, 2011; **Gholipour, *et al.***, 2012; **Landínez-Téllez, *et al.***, 2012). The RE3Ba5Cu8O18 unit cell was generated by this model and compared with each diffractogram after which we concluded that the model is consistent with the results. In this table, the space group, which corresponds to an orthorhombic structure *Pmm2* (25), the lattice parameters, the atomic position of each of the ions in the cell and its occupancy factor will be found.

Figure 2 shows the XRD patterns for the RE3Ba5Cu8O18 system at the room temperature obtained by the SSR method compared to the theoretical patterns of the RE-358 with the orthorhombic space group. All synthesized samples exhibited the reflections of the theorical phase. The difference in the synthesis temperature was expected as a result of crystallization temperatures of the RE-358 compounds changing the function of the ionic radius of RE3+ substituent ion (2). No change was evidenced in the positions of the XRD peaks for prepared samples indicating the absence of orthorhombic-tetragonal structural phase transition for RE-358, that is, no influence of the sintering temperature in the sintered compounds symmetry was observed (**Slimani, *et al.***, 2018; **Pavan-Kumar, *et al.***, 2018).

To confirm the crystalline structure, the XRD patterns were refined by the Rietveld method using the FullProf software program. The refined patterns are shown in **figures 3 and 4** for RE-358 with RE = Dy, Gd, Ho, Sm, Y, and Yb, respectively. In this graph, the experimental pattern is identified by the (•) symbol. The calculated pattern is the red line, the background is the green line, the experimental difference and calculated pattern is the blue line and the Bragg positions of each identified phase are shown in bars.

The coincidence between theoretical and experimental profiles confirmed that all samples had crystallized in an orthorhombic structure with Pmm2 (25) symmetry corresponding to the superconducting phase; the symmetries obtained matched with others reported by **Aliabadi, *et al.*** (2009), **Slimani, *et al.*** (2018), **Rekaby, *et al.*** (2018), and **Gholipour, *et al.*** (2012) and corroborated by the small values in the agreement parameters 2 y R(F2). The results showed that the crystalline structure was not lost when yttrium atoms were substituted with RE3+ trivalent ions. The non-superconducting RE-123 phase with P4/mmm tetragonal was identified in the RE-358 system. The structures of RE-358 consist of five CuO2 planes and three CuO chains (**Udomsamuthirun, *et al.***, 2010; **Ayas**, 2011). The presence of twin peaks 2θ ≈ 55.58° and 68.50° confirmed the orthorhombic nature of the RE-358 compound.

The a, b, and c values of RE-358 and RE-123 phases were in accord with previous reports by **Pavan-Kumar, *et al.*** (2018), **Udomsamuthirun, *et al.*** (2010), **Rekaby, *et al.*** (2014), **Gholipour, *et al.*** (2012) while the a and b lattice parameters of RE-358 were very similar to the RE-123 phase, although the c parameters were three times higher than the RE-123. The variations of lattice parameters and cell volume in the RE-358 phase as a function of atomic radius of the RE substituent ion are shown in **figure 3** where an increase in *a* and *c* lattice parameters and in cell volume as the atomic radius increased is evidenced. This may have been caused by the increase of the RE^{3+} ionic radius (ionic radius TR^{3+}). Increase in dimensions can be explained by the introduction of electrons in Cu-O orbitals on the *a-b* plane (**Ayas**, 2011).

Table 2. Theoretical model for the $RE_3Ba_5Cu_8O_{18}$ system

Lattice parameter			Space group
a (Å)	b (Å)	c (Å)	
3.8927	3.8303	32.0605	Pmm2
Atom	x	y	Z
RE	0.5000	0.5000	1.0000
Cu	0.0000	0.0000	0.0625
O	0.0000	0.5000	0.0625
O	0.5000	0.0000	0.0625
Ba	0.5000	0.5000	0.1250
O	0.0000	0.0000	0.1250
Cu	0.0000	0.0000	0.1875
O	0.0000	0.5000	0.1875
Ba	0.5000	0.5000	0.2500
O	0.0000	0.0000	0.2500
Cu	0.0000	0.0000	0.3125
O	0.0000	0.5000	0.3125
O	0.5000	0.0000	0.3125
RE	0.5000	0.5000	0.3750
Cu	0.0000	0.0000	0.4375
O	0.0000	0.5000	0.4375
O	0.5000	0.0000	0.4375
RE	0.5000	0.5000	0.5000
Cu	0.0000	0.0000	0.5625
O	0.0000	0.5000	0.5625
O	0.5000	0.0000	0.5625
Ba	0.5000	0.5000	0.6250
O	0.0000	0.0000	0.6250
Cu	0.0000	0.0000	0.6875
O	0.0000	0.5000	0.6875
Ba	0.5000	0.5000	0.7500
O	0.0000	0.0000	0.7500
Cu	0.0000	0.0000	0.8125
O	0.0000	0.5000	0.8125
Ba	0.5000	0.5000	0.8750
O	0.0000	0.0000	0.8750
Cu	0.0000	0.0000	0.9375
O	0.0000	0.5000	0.9375
O	0.5000	0.0000	0.9375

The samples were composed of both the superconducting and non-superconducting phases. The superconducting phase corresponds to the orthorhombic structure and the non-superconducting phase shows several crystal structures (**Table 3**). As reported by different authors, it is well known that the small reflections corresponding to a low amount of the non-superconducting phases are characteristics of these compounds since they are
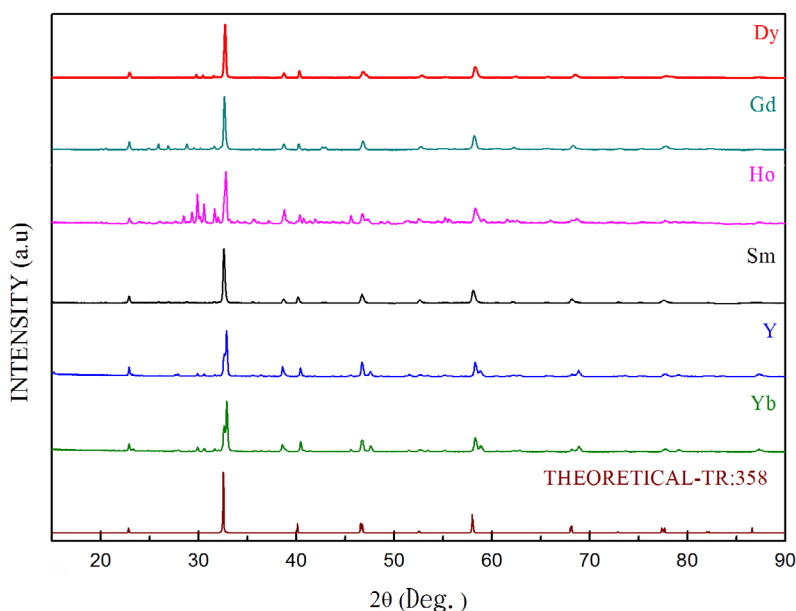
Figure 2. XRD patterns obtained for $RE_3Ba_5Cu_8O_{18}$ compounds.

crystalline structures thermally stable (**Aliabadi,** *et al.*, 2009; **Topal,** *et al.*, 2011). The lattice parameters of superconducting and non-superconducting phases are shown in **tables 4 and 5**. **Table 5** shows the percentage of the superconducting and non-superconducting phases in the samples. It is clear that the non-superconducting phase had a great contribution, except in the $Gd_3Ba_5Cu_8O_{18}$ sample. The Pmm2 space group corresponds to the superconducting phase while the other space groups of the non-superconducting phase are composed of P4/mmm (RE123), Pnma (RE211), and Im-3m ($BaCuO_2$), (see table 5). Based on more detailed DRX analyses, **Gholipour,** *et al.* (2012) and **Vovk** *et al.* (2008) demonstrated that the RE358 has two different structures: RE123 (P4/*mmm)* and RE358 (*Pmm2)* where the RE123 phase is dominant because the RE358 has a very complex crystalline network compared to the RE123 system due to the number of the CuO2 planes where the electrons are paired. Given the structural similarity of the two structures, it is difficult to produce the single-phase RE358 material and to distinguish them (**Gholipour,** *et al.,* 2012; **Dias,** *et al.,* 2014; **Topal,** *et al.,* 2011; **Vovk,** *et al.,* 2008; **Khosroabadi,** *et al.,* 2014). These results showed an increase in the percentage of the RE358 phase compared to other reports.

Figure 2 in the study by **Udomsamuthirun,** *et al.* (2010) shows a linear relation between the number of Cu-atoms in their sample versus the c-axis value in the XRD spectra (**Pimentel-Jr,** *et al.,* 2015). In our study, **figure 4a** shows the results found for our samples, which agree with those of **Sujinnapram,** *et al.* (2011).

Figures 4 (b,c) and 5 show a decreasing linear relationship of the orthorhombic unit cell parameter (a, b, V) in function of the rare earth ionic ratio $RE_3Ba_5Cu_8O_{18}$ samples; **Tarascón,** *et al.* (1987) suggested this is due to the removal of oxygen atoms from the copper atoms. From this perspective, the copper that was fourfold coordinated becomes twofold coordinated with an oxygen above and one below (**Sujinnapram,** *et al.,* 2011).

Figure 6 shows the ZFC and FC magnetization curves as a function of the temperature, which is typical of superconducting materials. The figure shows how the temperature Tc was extracted for each of the samples. The characteristic T_c divided the range of normal and superconducting phases showing the beginning of the diamagnetic characteristic contribution with values below the T_c ones, which were determined considering the intersection between the extrapolated magnetization in the normal and superconducting phases (**Supelano,** *et al.,* 2016).
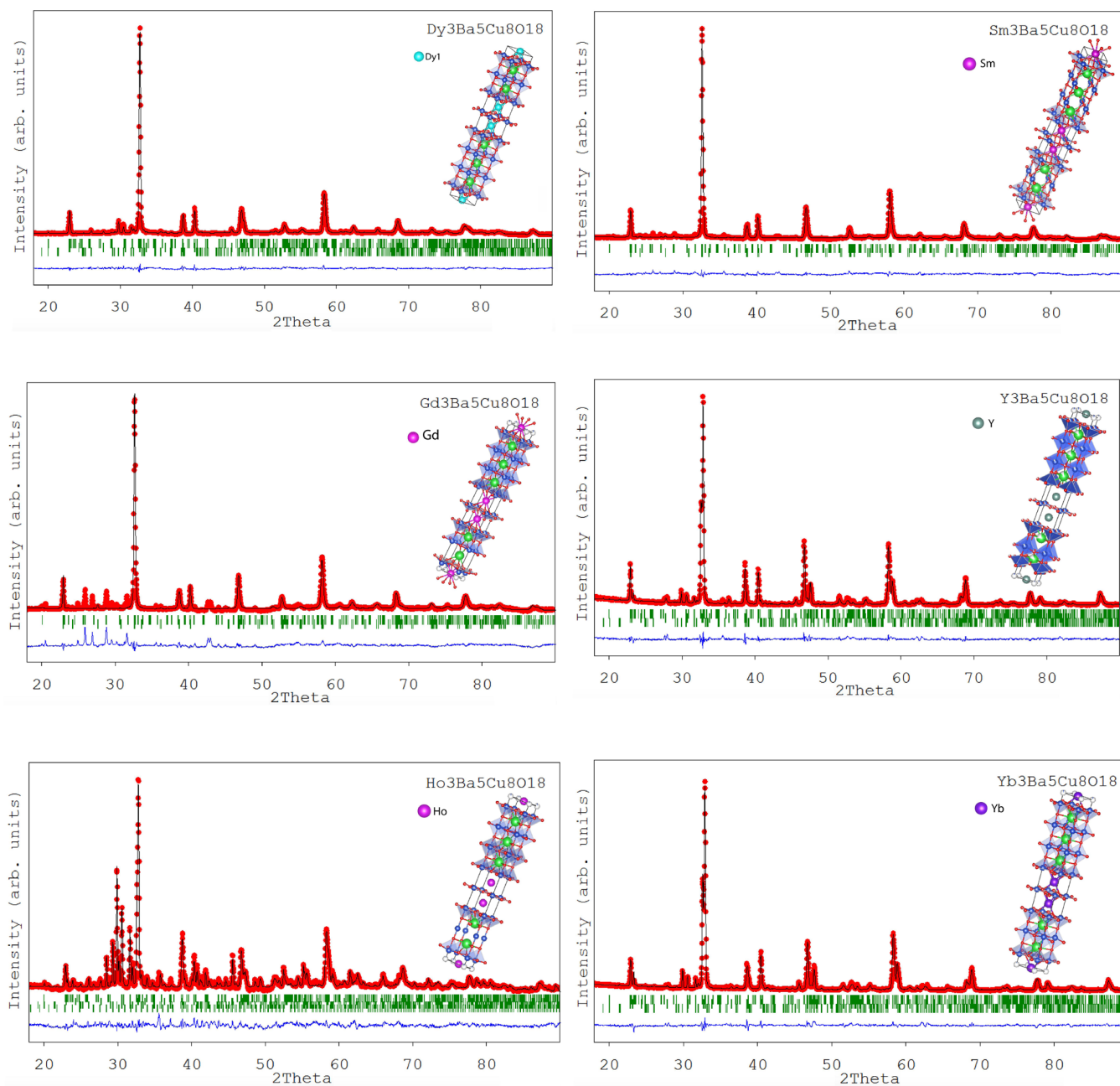
Figure 3. Rietveld refinements for $RE_3Ba_5Cu_8O_{18}$ (RE=Dy, Gd, and Ho). The red line corresponds to the experimental pattern, the black line to the calculated one, the green lines to the Bragg reflections, and the blue line shows the difference between the adjusted pattern and the experimental pattern.

The results obtained for the values of the critical temperature, all with an applied field of 100 Oe, are recorded in **table 3**. The materials exhibited a lower superconducting transition than Y-358 (**Aliabadi, et al.,** 2009) due to the change in the electronic structure of the sample since RE^{3+} has a larger ionic radius than Y demonstrating that an increase in the separation distance of the superconducting planes affects the T_c considerably, as well as the internal transfer of charges between the CuO_2 planes and the charge reservoirs thus causing the decrease of the T_c. This fact is in accordance with the decrease of the parameter c when the ionic radius of RE decreases, i.e., it represents the understanding of
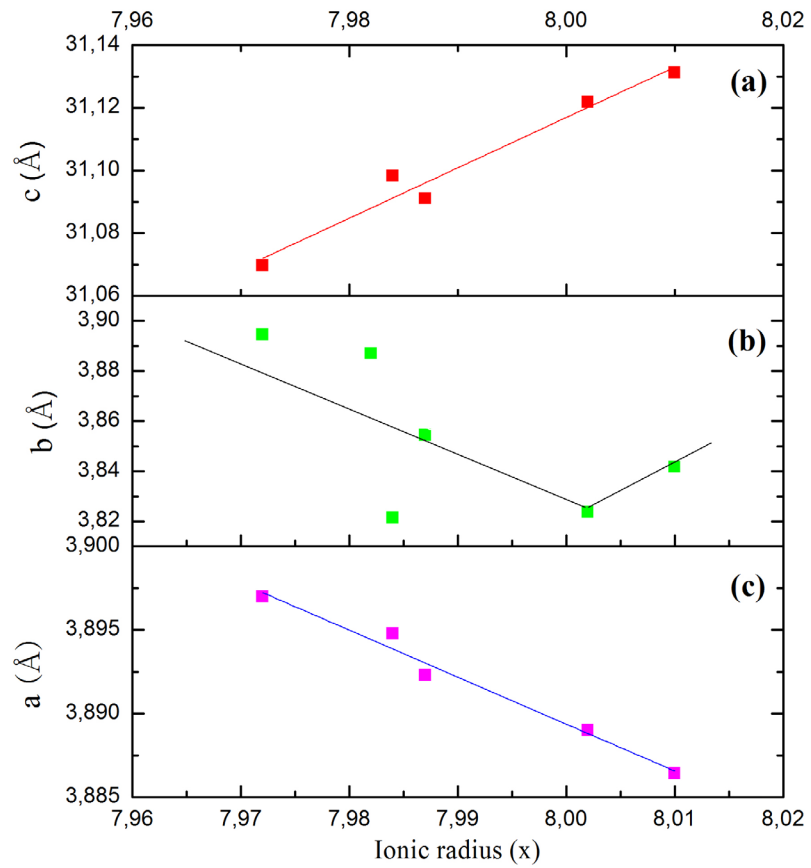
Figure 4. Orthorhombic unit cell parameter (a,b,c) as a function of the rare earth ionic ratio $RE_3Ba_5Cu_8O_{18}$ series for the as-prepared samples

Table 3. Lattice parameters of the superconducting phase in Pmm2 space group

System	χ^2	R (F^2)	a (Å)	b (Å)	c (Å)	α	β	γ	R_{wp}	R_{exp}	Anis	c/a ratio
$Dy_3Ba_5Cu_8O_{18}$	1.977	0.330	3.892(3)	3.854(4)	31.091(1)	90	90	90	15.20	7.69	0.978	7.987
$Gd_3Ba_5Cu_8O_{18}$	4.444	0.087	3.887(8)	3.887(0)	31.035(4)	90	90	90	36.80	8.28	0.020	7.982
$Ho_3Ba_5Cu_8O_{18}$	2.480	0.231	3.886(4)	3.841(7)	31.131(3)	90	90	90	22.00	8.86	1.156	8.010
$Sm_3Ba_5Cu_8O_{18}$	2.439	0.191	3.897(0)	3.894(4)	31.069(7)	90	90	90	19.05	7.81	0.066	7.972
$Y_3Ba_5Cu_8O_{18}$	2.260	0.355	3.889(0)	3.823(7)	31.121(9)	90	90	90	17.20	7.61	1.693	8.002
$Yb_3Ba_5Cu_8O_{18}$	2.197	0.283	3.894(8)	3.821(5)	31.098(3)	90	90	90	16.30	7.42	1.899	7.984

the c axis and causes a reduction in the density of states in the Fermi energy which leads to the reduction of the T_c. This may be attributed to the concentration in the basal plane due to the reduction of vacancies or oxygen sites in the CuO_2 planes. In general, there is a critical-temperature dependence on the ionic radius of the substituent ion RE since the critical temperatures tend to be higher as the RE ionic radius approaches the Y ionic radius. This behavior regarding the ionic radius and T_c alone is different in Ho-358. It is important to note that the Pnma (RE211) and Im-3m ($BaCuO_2$) non-superconducting phases have no magnetic response and that its training is due to the synthesis method used, which is typical for 358 systems because they are thermally stable crystal structures (**Gholipour,** *et al.***,** 2012; **Supelano,** *et al.***,** 2014).

**Table 4.** Percentage of the phase composition and the critical temperature

| Samples | Percentage of the phase composition (%) | | | | |
| | Superconducting phase | Non-superconducting phase | | | |
	RE358, Pmm2	RE123, P4/mmm	RE211, Pnma	BaCuO$_2$, Im-3m	Tc (K)
Dy$_3$Ba$_5$Cu$_8$O$_{18}$	26.81	67.21	5.98		90
Gd$_3$Ba$_5$Cu$_8$O$_{18}$	59.88	40.12			80
Ho$_3$Ba$_5$Cu$_8$O$_{18}$	15.31	34.32	20.62	29.75	91
Sm$_3$Ba$_5$Cu$_8$O$_{18}$	41.69	58.31			93
Y$_3$Ba$_5$Cu$_8$O$_{18}$	30.04	66.84	3.12		95
Yb$_3$Ba$_5$Cu$_8$O$_{18}$	37.91	57.79	4.30		94

Table 5. Lattice parameters of the non-superconducting phase

| | Non-superconducting phase | | | | | | | | |
| | RE123, P4/mmm | | | RE211, Pnma | | | BaCuO$_2$, Im-3m | | |
Samples	a (Å)	b (Å)	c (Å)	a (Å)	b (Å)	c (Å)	a (Å)	b (Å)	c (Å)
Dy$_3$Ba$_5$Cu$_8$O$_{18}$	3.874(4)	3.874(4)	11.642(5)	12.238(4)	5.679(0)	7.156(6)	-	-	-
Gd$_3$Ba$_5$Cu$_8$O$_{18}$	3.883(0)	3.883(0)	11.628(9)	-	-	-	-	-	-
Ho$_3$Ba$_5$Cu$_8$O$_{18}$	3.869(5)	3.869(5)	11.630(5)	12.178(5)	5.661(7)	7.131(4)	18.298(8)	18.298(8)	18.298(8)
Sm$_3$Ba$_5$Cu$_8$O$_{18}$	3.889(0)	3.889(0)	11.633(8)	-	-	-	-	-	-
Y$_3$Ba$_5$Cu$_8$O$_{18}$	3.855(2)	3.855(2)	11.670(0)	12.174(0)	5.657(1)	7.128(6)	-	-	-
Yb$_3$Ba$_5$Cu$_8$O$_{18}$	3.848(0)	3.848(0)	11.681(3)	12.179(1)	5.661(3)	7.133(4)	-	-	-
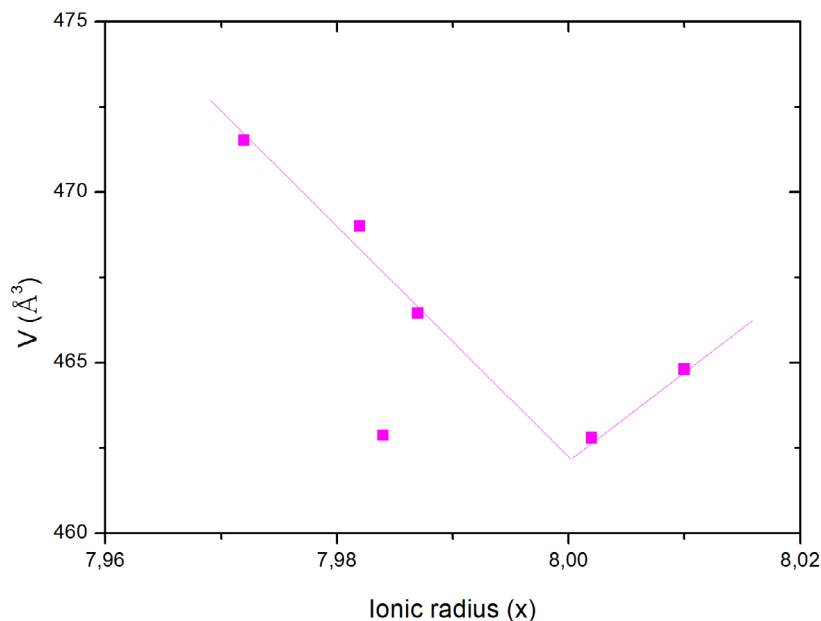
Figure 5. Orthorhombic unit cell parameter (V) as a function the rare earth ionic ratio $RE_3Ba_5Cu_8O_{18}$
series for the as-prepared samples
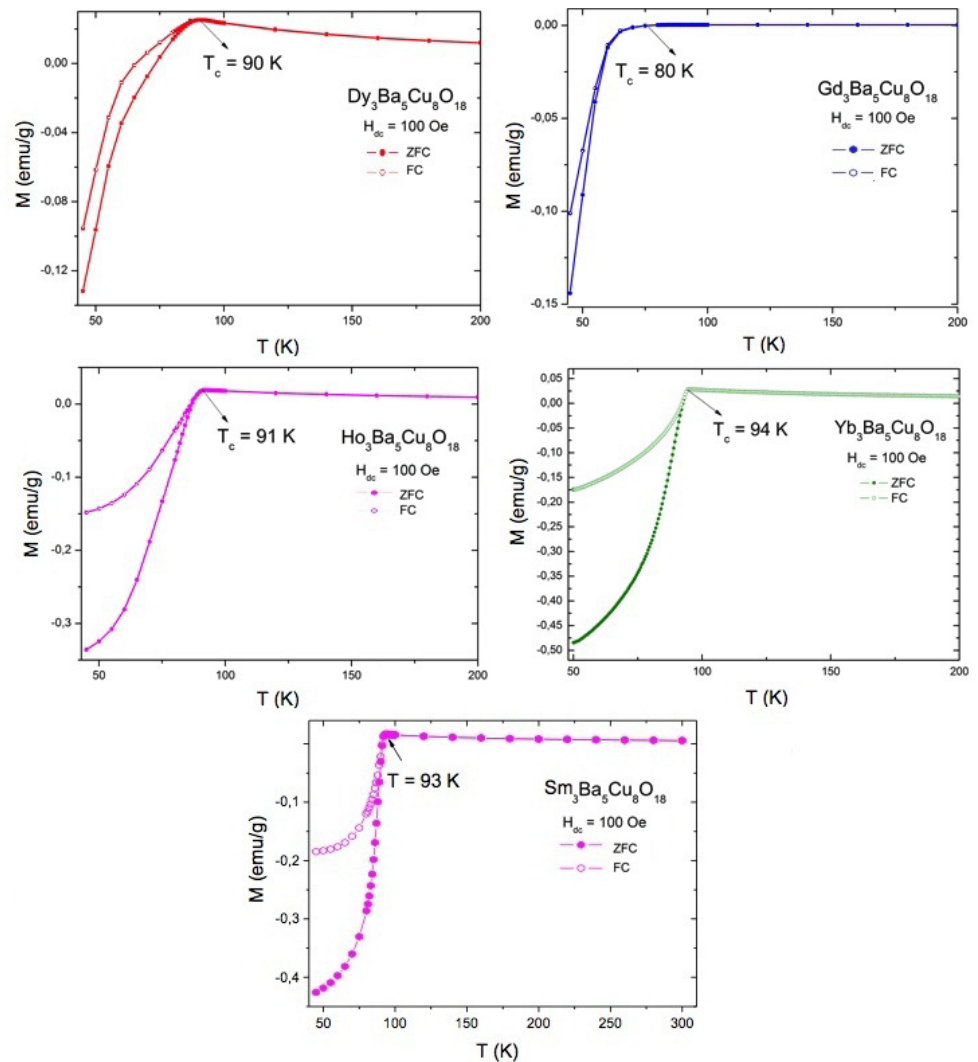
Figure 6. Magnetization versus temperature for the $RE_3Ba_5Cu_8O_{18}$ systems

Conclusions

We produced the $RE_3Ba_5Cu_8O_{18-\delta}$ (RE = Sm, Eu, Gd, Dy, Ho) superconducting system using the solid-state reaction method. We studied the XRD spectra of the $RE_3Ba_5Cu_8O_{18}$ superconductors with the Rietveld method to determine the phase composition, lattice parameters, and space group of the superconducting and non-superconducting phases. The Pmm2 space group corresponded to the superconducting phase while *P4/mmm* (RE123), *Pnma* (RE211), and *Im-3m* (BaCuO2) corresponded to the other space groups of the non-superconducting phase. The more non-superconducting phases are present, the more anisotropy parameters are found.

The high Tc $RE_3Ba_5Cu_8O_{18}$ superconductor compounds studied here had a crystal structure like Y123 with the exception of the number of CuO chains and CuO_2 planes, which exceed those in Y123. The $RE_3Ba_5Cu_8O_{18}$ has five CuO_2 planes and three CuO chains. It seems that increasing the number of the CuO_2 planes and the position of the CuO chains has important effects on the value of the transition temperature in the $RE_3Ba_5Cu_8O_{18}$ compounds. Magnetization measurements demonstrated the wide characteristics of the $RE_3Ba_5Cu_8O_{18}$ superconductor system. The critical temperature of the $RE_3Ba_5Cu_8O_{18}$ samples ranged from 80 to 95 K depending on the rare earth.

Author contributions

CAPV oversaw the production of samples and the writing of the document; CC carried out the analysis and interpretation of the results and elaborated the figures and tables; JRR was responsible for the style correction and the review of the final document; JAA collaborated in the analysis and interpretation of the results.

Conflicts of interest

The authors declare that there is no conflict of interests of any kind regarding the publication of the results of our research work.

References

Aliabadi, A., Farshchi, Y.A., Akhavan, M. (2009). A new Y-based HTSC with Tc above 100 K. Physica C. **469:** 2012-2014.

Ayas, O. (2011). The Structural, Superconducting and Transport Properties of the Compounds $Y_3Ba_5Cu_8O_{18}$ and $Y_3Ba_5Ca_2Cu_8O_{18}$. J. Supercond. Nov. Magn. **24:** 2243-2252.

Dias, F.T., Oliveira C.P., Vieira, V.N., Silva D.L., Mesquita, F., Almeida, M.L., Schaf, J., Pureur, P. (2014). Magnetic irreversibility and zero resistance in granular Y358 superconductor. Journal of Physics Conference Series. **568:** 1-5.

Gholipour, S., Daadmehr, V., Rezakhani, A.T., Khosroabadi, H., Shahbaz-Tehrani, F., Hosseini-Akbarnejad, R. (2012). Structural Phase of Y358 Superconductor Comparison with Y123. J. Supercond. Nov. Magn. **25:** 2253-2258.

Khosroabadi, H., Rasti, M., Akhavan, M. (2014). Structural analysis of Y3Ba5Cu8O19−δ high-Tc superconductor by ab initio density functional theory. Phys. C Supercond. **497:** 84-88.

Landínez-Téllez, D.A., Cabrera-Báez, M., Roa-Rojas, J. (2012). Structure and conductivity fluctuations of the $Y_3Ba_5Cu_8O_{18}$ superconductor. Modern Physics Letters B. **26:** 1-11.

Pavan-Kumar, S., Santosh, M., Swarup-Raju, P.M. (2018). Structural and Thermal Validations of $Y_3Ba_5Cu_8O_{18}$ Composites Synthesized via Citrate Sol-Gel Spontaneous Combustion Method. J. Supercond. Nov. Magn. **31:** 1279-1286.

Peña, J.P., Martínez, D.B., Parra-Vargas, C.A. (2013). Magnetic Measurements and Kinetic Energy of the Superconducting Condensate in $SmBa_2Cu_3O_{7-\delta}$. Brazilian J. Phys. **43:** 22-27.

Pimentel-Jr, J. L., Martínez-Buitrago, D., Supelano, I., Parra-Vargas, C. A., Mesquita, F. R., Pureur, P. (2015). Synthesis and Characterization of the Superconductors $Y_3Ba_5Cu_{8-x}Fe_xO_{18}$ (0.0597 ≤ x ≤ 0.1255). Journal of Superconductivity and Novel Magnetism. **28:** 509-512.

Rekaby, M., Roumié, M., Abou-Aly, A., Awad, R., Yousry, M. (2014). Magnetoresistance Study of $Y_3Ba_5Cu_8O_{18}$ Superconducting Phase Substituted by Nd^{3+} and Ca^{2+} Ions. J. Supercond. Nov. Magn. **27:** 2385-2395.

Sandoval-Gutiérrez, S., Supelano, G.I., Roa-Rojas J., Parra-Vargas, C.A. (2015). Production a characterization of new system superconductor $TR_3Ba_8Cu_{11}O_\delta$. Journal of Physics: Conference Series. **687:** 1-4.

Sujinnapram, S., Udomsamuthirum, P., Kruaehong, T., Nilkamjon T., Ratreng S. (2011). XRD spectra of new YBaCuO superconductors. Bull. Meter. Sci. **34:** 1053-1057.

Slimani, Y., Hannachi, E., Zouaoui, M., Ben-Azzouz, F. (2018). Excess Conductivity Investigation of $Y_3Ba_5Cu_8O_{18\pm\delta}$ Superconductors Prepared by Various Parameters of Planetary Ball Milling Technique. J. Supercond. Nov. Magn. **31:** 2339-2348.

Supelano, G.I., Pimentel, J.L., Palacio, C.A., Mejía-Gómez, J.A., Menegotto-Costa, R., Caicedo-Mateus, F., Martínez-Buitrago, D., Roa-Rojas, J., Mesquita, F., Parra-Vargas, C.A. (2016). Weak Field Magnetic Susceptibility Fluctuations Above the Superconducting Transition $YBa_2Cu_{3-x}FexO_{7-\delta}$ (0.05 ≤ x ≤ 0.12). J. Low Temp. Phys. **182:** 141-152.

Supelano, G.I., Sarmiento-Santos, A., Parra-Vargas, C.A. (2014). Magnetic fluctuations on $TR_3Ba_5Cu_8O_8$ (TR=Ho, Y and Yb) superconducting system. Phys. B Condens Matter. **455:** 79-81.

Tarascón, J.M., McKinnon, W.R., Greene, L.H., Hull, G.W., Vogel, E.M. (1987). Oxygen and rare-earth doping of the 90 K superconducting perovskite $YBa_2Cu_3O_{7-x}$. Physical Review B. **36:** 226-234.

Tavana A. & Akhavan M. (2010). How T_c can go above 100 K in the YBCO family. The European Physical Journal B. **73:** 79-83.

Topal, U. & Akdogan, M. (2012). The Role of Oxygenation on Superconducting Properties of RE$_3$Ba$_5$Cu$_8$O$_{18}$ (RE =Y, Sm and Nd) Compounds. J. Supercond. Nov. Magn. **25:** 239-244.

Topal, U., Akdogan, M., Ozkan, H. (2011). Electrical and Structural Properties of RE3Ba5Cu8O18 (RE=Y, Sm and Nd) Superconductors. J. Supercond. Nov. Magn. **24:** 2099-2102.

Udomsamuthirun, P., Kruaehong, T., Nilkamjon, T., Ratreng, S. (2010). The New Superconductors of YBaCuO Materials. J Supercond Nov Magn. **23:** 1377-1380.

Vovk, R.V. (2008). Effect of high pressure on the fluctuation conductivity and the charge transfer of YBa2Cu3O7−δ single crystals. J. Alloys Compd. **453:** 69-74.

Wu, K., Ashburn, J.R., Torng, C.J., Hor, P.H., Meng, R.L., Gao, L., Huang, Z.J., Wang, Y.Q., Chu, C.W. (1987). Superconductivity at 93 K in a new mixed-phase Y-Ba-Cu-O compound system at ambient pressure. Phys. Rev. Lett. **58:** 908.